ACR No. L5K05

NATIONAL ADVISORY COMMITTEE FOR AERONAUTICS

WARTIME REPORT

ORIGINALLY ISSUED
February 1946 as
Advance Confidential Report L5K05

DETERMINATION OF THE STABILITY AND CONTROL CHARACTERISTICS OF A STRAIGHT-WING, TAILLESS FIGHTER-AIRPLANE MODEL IN THE LANGLEY FREE-FLIGHT TUNNEL

By Charles L. Seacord, Jr. and Herman O. Ankenbruck

Langley Memorial Aeronautical Laboratory
Langley Field, Va.

WASHINGTON

NACA ACR No. L5K05

NATIONAL ADVISORY COMMITTEE FOR AERONAUTICS

ADVANCE CONFIDENTIAL REPORT

DETERMINATION OF THE STABILITY AND CONTROL CHARACTERISTICS OF A STRAIGHT-WING, TAILLESS FIGHTER-AIRPLANE MODEL IN THE LANGLEY FREE-FLIGHT TUNNEL

By Charles L. Seacord, Jr. and Herman O. Ankenbruck

SUMMARY

An investigation to determine the stability and control characteristics of a straight-wing, tailless fighter model with a pusher propeller designed by the NACA has been made in the Langley free-flight tunnel. The investigation consisted principally of force and flight tests of a powered dynamic model. The effects of tail configuration, center-of-gravity location, and power on the stability and control characteristics of the model were determined. Tests were also made in the Langley 15-foot free-spinning tunnel to determine whether the model would trim at very high angles of attack.

The results of the investigation may be summarized as follows: The general flight characteristics of the model were good and compared favorably with the flight characteristics of good conventional airplane models previously tested in the Langley free-flight tunnel. As the angle of attack was increased, the longitudinal stability of the model increased instead of decreasing as that of tailless airplanes with swept-back wings usually does. Power caused a slight reduction in the longitudinal stability measured at constant power. This reduction in stability, however, did not affect the longitudinal steadiness of the model in flight tests. The model did not show the tendency to trim at very high angles of attack (above the stall) that has been a characteristic of some swept-back tailless airplanes. The lateral flight characteristics of the model with both vertical tails installed were good. The directional stability of the model was satisfactory and was improved by the application of power. The effective dihedral was desirably small and was not appreciably affected by power.

The control surfaces of the model provided adequate longitudinal and lateral control.

INTRODUCTION

Previous investigations of the stability and control of tailless airplanes with sweepback (references 1 to 4) have indicated that the sweepback is the cause of the poor longitudinal stability and the loss of control near the stall which are often characteristic of such airplanes. In order to determine the effects on stability of eliminating the sweepback, a straight-wing, tailless fighter airplane has been designed by the NACA and a model of the design has been tested in the Langley free-flight tunnel.

The present investigation is one phase of the tailless-airplane research program being carried out in the Langley free-flight tunnel to determine the relative merits of the various types of tailless aircraft and includes results of both force and flight tests of a dynamic powered model with a pusher propeller. Because some tendency has been noted for tailless airplanes to trim at very high angles of attack, $\pm 90^{\circ}$, brief tests were also made in the Langley 15-foot free-spinning tunnel to investigate the trim characteristics of the model at large angles of attack. The force tests were made with the model equipped with two different sizes of vertical tail surface, with propellers off and with propellers on, and with power adjusted to simulate that typical of modern fighter airplanes. The model was flown with two different sizes of vertical tail, with various center-of-gravity locations, and with various amounts of power.

SYMBOLS AND DESIGNATIONS

C_L lift coefficient $\left(\frac{\text{Lift}}{qS}\right)$

C_D drag coefficient $\left(\frac{\text{Drag}}{qS}\right)$

$C_{m_{c.g.}}$ pitching-moment coefficient about normal center-of-gravity location $\left(M/q\bar{c}S\right)$

C_Y lateral-force coefficient $\left(\frac{\text{Lateral force}}{qS}\right)$

C_l rolling-moment coefficient (L/qbS)

C_n yawing-moment coefficient (N/qbS)

L rolling moment, foot-pounds

M pitching moment, foot-pounds

N yawing moment, foot-pounds

q dynamic pressure, pounds per square foot $\left(\frac{1}{2}\rho V^2\right)$

ρ mass density of air, slugs per cubic foot

V airspeed, feet per second

W weight of airplane, pounds

S wing area, square feet

b wing span, feet

c wing chord, inches

$\bar{c}$ mean aerodynamic chord (M.A.C.), feet

α angle of attack of fuselage reference line, degrees

ψ angle of yaw, degrees ($\psi = -\beta$)

β angle of sideslip, degrees

ϕ angle of roll, degrees

C_{l_β} rate of change of rolling-moment coefficient with angle of sideslip, per degree $\left(dC_l/d\beta\right)$

C_{n_β} rate of change of yawing-moment coefficient with angle of sideslip, per degree $\left(dC_n/d\beta\right)$

T_c thrust disk-loading coefficient $\left(T/\rho V^2 D^2\right)$

T thrust, pounds

D propeller diameter, feet

δ_{a_R} right-aileron deflection, degrees

δ_e elevator deflection, degrees

k_X radius of gyration about X-axis

k_Y radius of gyration about Y-axis

k_Z radius of gyration about Z-axis

The parts of the model are designated as follows:

W wing

F fuselage, including pilot's enclosure and wire landing gear

P propeller

V_1 lower vertical tail

V_2 upper vertical tail

APPARATUS

Wind Tunnels

The investigation was carried out in the Langley free-flight tunnel, which is equipped for testing free-flying dynamic models. A complete description of the tunnel and its operation is given in reference 5. Force measurements were made on the Langley free-flight-tunnel six-component balance described in reference 6. The forces and moments are measured on this balance with respect to stability axes. The stability axes of an airplane are defined as an orthogonal system of axes intersecting at the center of gravity in which the Z-axis is in the plane of symmetry and perpendicular to the relative wind, the X-axis is in the plane of symmetry and perpendicular to the Z-axis, and the Y-axis is perpendicular to the plane of symmetry. A sketch showing the stability axes of an airplane is presented as figure 1. A photograph of the test section of the tunnel showing the model being tested in flight is presented as figure 2. The tests to determine the trim characteristics of the model at high angles of attack were made in the Langley 15-foot free-spinning tunnel, a description of which is given in reference 7.

Model

The test model was designed and constructed by the NACA and corresponds to a $\frac{1}{10}$-scale model of a hypothetical tailless airplane with a 40-foot span. It is a high-wing design with the 50-percent-chord line straight and has a small fuselage, a pusher propeller, and conventional vertical tail surfaces. A drawing and photographs of the model are given as figures 3 to 6.

Longitudinal control for the model was provided by elevators that extended over the inboard portion of the wing, and lateral control was provided by conventional aileron and rudder surfaces. For power-off (windmilling) tests, the model was fitted with a four-blade propeller that was allowed to windmill freely. For power-on tests, the model was equipped with a $\frac{1}{2}$-horsepower electric motor driving an 11-inch-diameter three-blade propeller. The three-blade propeller was installed in place of the four-blade propeller because the characteristics of the motor made it possible to obtain higher thrusts with this arrangement.

The model wing had a Rhode St. Genese 35 airfoil section (reflexed) because this section has a high maximum lift coefficient at the low Reynolds numbers at which the tests were run.

The physical characterististics of a full-scale airplane based on scaled-up values (10:1) of the dimensions of the model are:

Weight, pounds	8030
Wing	
Area, square feet	266.67
Span, feet	40.0
Aspect ratio	6.0
Sweepback of 50-percent-chord line, degrees	0
Sweepback of 25-percent-chord line, degrees	3.2
Incidence, degrees	0
Dihedral angle of midthickness line, degrees	0
Taper ratio	2:1
M.A.C., inches	83.9
Location of M.A.C. behind L.E. of root chord, inches	12.0
Root chord, inches	107.8
Tip chord, inches	53.9

Wing loading, W/S, pounds per square foot	30
Aileron	
Type	Plain
Area, percent wing area	7
Span, percent wing span	45
Chord, percent wing chord	20
Elevator	
Type	Plain flap
Area, percent wing area	7.7
Span, percent wing span	45
Chord, percent wing chord	15
Normal c.g. location	
Behind L.E. of root chord, inches	28.8
Behind L.E. of root chord, percent M.A.C.	20.0
Above thrust line, inches	4.0
Above thrust line, percent M.A.C.	4.8
Ratios of radii of gyration to wing span	
k_X/b	0.158
k_Y/b	0.133
k_Z/b	0.173
Vertical tails	
Total area of each, percent wing area	3.0
Rudder area, percent total vertical-tail area	23
Aspect ratio (each tail)	1.85
Distance from c.g. to rudder hinge line, percent wing span	24.2

TESTS

Force Tests

Most of the force tests were made at a dynamic pressure of 4.09 pounds per square foot, which corresponds to a test Reynolds number of approximately 240,000 based on the mean aerodynamic chord of 0.699 foot. The force tests consisted of angle-of-attack runs made to determine the effects of power and various modifications to the model on longitudinal stability and control and yaw runs made to determine the lateral stability and control characteristics of the model in all conditions. A summary of the force-test conditions is given in table I. As shown in table I, power-on force tests were made to determine the static longitudinal stability of the model operating with power simulating zero thrust and 1200 brake horsepower for the hypothetical full-scale airplane. In the lateral-stability tests the model operated with power simulating

zero thrust, 1200 brake horsepower, and 2000 brake horsepower for the full-scale airplane.

Values of thrust coefficient required to simulate 1200 and 2000 brake horsepower over the lift range of the model tests are shown in figure 7. These data are based on an assumed propeller efficiency for the full-scale airplane of 75 percent and a wing loading of 30 pounds per square foot.

Flight Tests

Model flight tests were made to determine effects of lift coefficient, center-of-gravity location, vertical-tail area, and power on the stability and control characteristics of the model. In the power-off condition, flights were made over a range of lift coefficients from 0.32 to 0.95 for center-of-gravity locations ranging between 15 and 23 percent M.A.C. Most flight tests were made with the model equipped with both upper and lower vertical tails, but a few tests were made with the model equipped with the upper tail only. Power-on flight tests were made for a lift-coefficient range with the normal center-of-gravity location (20 percent M.A.C.). The highest power simulated in flight was 1200 brake horsepower.

Free-to-Trim Tests

In the free-to-trim tests the model was supported in the air stream of the Langley 15-foot free-spinning tunnel on the stand shown in figure 8. The model was free to rotate in pitch about its center of gravity and had a possible travel of about 200°. The model was restrained until the airspeed had been adjusted and was then released to trim. The model was released at angles of attack from 0° to ± 90° with the elevators set to trim the model at an angle of attack of 8°.

RESULTS AND DISCUSSION

Longitudinal Stability

Power-off force tests.- The results of force tests made to determine the longitudinal stability characteristics

of the model with power off are presented in figure 9. The effects of the various component parts of the model on the stability are also shown in this figure.

The data of figure 9 show that the model was longitudinally stable up to the stall. This characteristic is desirable and is not usually possessed by tailless designs incorporating sweepback. The stability of the model increased with increasing lift coefficient; the static margin, as indicated by the value of $-dC_m/dC_L$, varied from about 0.02 at low lift coefficients to about 0.07 at high lift coefficients with the normal center-of-gravity location (20 percent M.A.C.). Reference 8 shows that this change in the slope of the pitching-moment curve is characteristic of a high-wing arrangement on a round fuselage and indicates that the pitching-moment curve could probably be straightened by lowering the wing to a high midwing position.

The data of figure 9 show that adding the fuselage to the wing caused a reduction in static margin $\left(-dC_m/dC_L\right)$ of about 0.01. The data also show, however, that the stabilizing effect of the windmilling pusher propeller counteracted the destabilizing fuselage effect, so that the stability of the complete model was similar to that of the wing alone.

Power-off flight tests.- In power-off flight tests with the center of gravity at 20 percent M.A.C., the longitudinal stability of the model was satisfactory at lift coefficients from 0.50 to the stall, at which the static margin was 0.05. At lift coefficients less than 0.50, however, the longitudinal motion of the model was unsteady and frequent elevator control was required to keep the model flying. This unsteadiness was attributed to the small static margin (about 0.02 or 0.03) at low lift coefficients previously indicated by the force tests.

When the static margin was increased by 0.02 by moving the center of gravity ahead to 18 percent M.A.C., steady flights were obtained over the entire lift range from a lift coefficient of 0.32 to the stall (flights could not be made at lift coefficients lower than 0.32 because of tunnel airspeed limitations).

Decreasing the static margin by shifting the center of gravity to 22 percent M.A.C. caused the longitudinal

flight behavior of the model to become completely unsatisfactory at lift coefficients less than 0.50 and only fairly satisfactory at lift coefficients greater than 0.50. In some flights made at lift coefficients above 0.50 with a static margin of about 0.02 or 0.03, the model was very unsteady and difficult to control and the longitudinal characteristics were very similar to those obtained in the flight tests made at lift coefficients below 0.50 and with the center of gravity at 20 percent M.A.C.

Previous tests in the Langley free-flight tunnel (reference 9) have shown that conventional models had longitudinal steadiness characteristics which were essentially the same as those of the straight-wing, tailless model with corresponding values of static margin. In this respect the results of the present investigation are in agreement with the results of reference 9, which showed that variation of damping in pitch has little effect on longitudinal steadiness as long as the static margin is satisfactory.

Power-on force tests.- For purposes of discussion, static margin has been assumed equal to $-dC_m/dC_L$. This assumption should be nearly true in the case of the model tested because the model has no horizontal tail and because the wing is not in the slipstream. The force-test data of figure 10 show that power caused a reduction in static margin which, though appreciable (0.03 or 0.04), was not so great as the reduction often caused by power on conventional single-engine airplanes with tractor propellers (reference 10). At 1200 brake horsepower with the center of gravity at 20 percent M.A.C. the model had a static margin of only about 0.01 over most of the lift range.

The results of calculations made to determine the cause of the decrease in stability with application of power are presented in figure 11 in the form of incremental pitching moments provided by the propeller normal force and propeller thrust (figs. 11(a) and (b)). The combined calculated effects of propeller forces are also compared (fig. 11(c)) with the measured power effects taken from the data of figure 10. The calculations show that, although the normal force of the pusher propeller provided a slight stabilizing effect, the propeller thrust provided a much greater destabilizing effect. Figure 11 shows that the measured destabilizing effect of power was about twice the calculated effect of direct propeller

forces. The additional unstable moments may have been produced by the inflow effects over the wing and the rear portion of the fuselage. The data of figure 12 show that if the center of gravity of the model were shifted vertically downward from 0.048 M.A.C. above the thrust line to 0.011 M.A.C. below the thrust line, power would not affect the static longitudinal stability of the model.

Power-on flight tests.- Although the force-test results indicated a decrease in longitudinal stability to a static margin of 0.01 as the power was increased from zero thrust to 1200 brake horsepower, the longitudinal steadiness in flight tests of the model was not appreciably changed by power application. Flights made with power simulating 1200 brake horsepower were as steady as flights made with zero thrust. These results thus appear to disagree with the results of the power-off flight tests, in which a reduction of the power-off static margin from 0.05 to 0.02 caused the longitudinal steadiness of the model to become definitely worse.

An explanation of this apparent discrepancy is that in the power-on force tests the thrust was varied with angle of attack to represent constant-power flight at different airspeeds - that is, T_c was varied with C_L and thus with airspeed, as shown in figure 7 - whereas in the power-on flight tests the airspeed did not vary immediately with angle-of-attack changes - that is, T_c and airspeed remained constant when the model pitched up or down. If the thrust coefficient T_c instead of the power had been kept constant in the force tests, there would likely have been little or no change in stability from the zero-thrust to the power-on conditions. The assumption is here made that curves of pitching-moment coefficient against lift coefficient at constant thrust coefficient would have remained parallel for any value of thrust coefficient; that is,

$$\left(\frac{dC_m}{dC_L}\right)_{T_c=0} = \left(\frac{dC_m}{dC_L}\right)_{T_c = \text{Any value}}$$

Since longitudinal steadiness is largely dependent on the rapid pitching motions or short-period oscillations that cause no appreciable change in airspeed, the steadiness appears to be affected principally by stability changes that occur at conditions of constant thrust coefficient and constant airspeed and very little by changes that occur at conditions of constant power and varying airspeed.

Longitudinal Control

The longitudinal-control data obtained in the force tests are shown in figure 10. These data indicate that with the normal center-of-gravity location the model could be trimmed from zero lift coefficient to maximum lift coefficient with a total elevator movement of about 20°. The elevator effectiveness did not change noticeably when power was applied, which indicated that there was little effect of induced flow over the elevators. Flight tests showed that the elevator was powerful enough to trim the model over the entire flight range with the center of gravity at 18 percent M.A.C.

Trim at High Angles of Attack

In the free-to-trim tests in the Langley 15-foot free-spinning tunnel, the model upon being released in the upright or inverted position (at angles of attack of 90° or -90°) assumed immediately the angle of attack for which the elevators had been set, 8°. Under no conditions did the model show the tendency to trim at high angles of attack that has been exhibited by some swept-back tailless designs.

Lateral Stability

Force tests.- The results of tests made to determine the lateral stability characteristics of the model are presented in figures 13 and 14. These results are summarized in figure 15 in the form of a stability chart that is a plot of the directional-stability parameter C_{n_β} against the effective-dihedral parameter C_{l_β}.

The data of figures 13 and 15 show the effect of the various component parts of the model on lateral stability. The wing-fuselage combination had slight directional instability but was made slightly stable by the addition of the pusher propeller. Addition of the vertical tails increased the directional stability with propeller windmilling to a value of C_{n_β} of about 0.0007. The effective dihedral was small for all conditions, about 2° for the wing-fuselage combination and about 1° for the complete model.

The force-test data of figures 14 and 15 show a noticeable increase in directional stability with application of power. Increasing the power from idling to 2000 brake horsepower increased the directional stability by approximately 65 percent. The data of figure 14 also show that applying power with the vertical tails off did not increase the directional stability appreciably. The increase in directional stability at high power with tails on appears to be caused primarily by the inflow effects upon the vertical tails rather than from action of the direct propeller forces. The effective dihedral was apparently not affected by an increase in power. (See figs. 14 and 15.)

Flight tests.- The lateral flight characteristics of the model with both vertical tails installed were good for powers ranging from zero thrust to 1200 brake horsepower. The directional stability appeared to be satisfactory in flights at zero thrust and improved with the application of power. The small effective dihedral shown by the force tests was noted in the flights by the absence of any appreciable rolling motions when the model was disturbed in yaw and by the negligible effects on aileron control of the adverse yawing produced in rolling maneuvers. This small effective dihedral was considered a desirable characteristic for a tailless design because of the relatively low directional stability of this type of airplane.

In flights with the lower tail removed, the lateral flight characteristics were not so good as those with both tails installed. The adverse yawing due to aileron control was greater and the yawing motions of the model damped out more slowly after disturbances in yaw. The lateral flight characteristics were considered not quite satisfactory with this tail configuration.

Lateral Control

The force-test data showing the aileron effectiveness are presented in figure 16. These data show that the ailerons were effective at all angles of attack up to the stall (approx. 12°).

In the flight tests adequate lateral control was obtained by using abrupt aileron deflections of ± 15°. Rudder deflections of ± 12° used in conjunction with the

aileron control were usually sufficient to balance out the adverse yawing moments caused by aileron deflection and rolling velocity.

CONCLUSIONS

The results of tests in the Langley free-flight tunnel of a straight-wing, tailless fighter model with a pusher propeller may be summarized as follows:

1. The general flight characteristics of the model were good and compared favorably with the flight characteristics of good conventional airplane models previously tested in the Langley free-flight tunnel.

2. As the angle of attack was increased, the longitudinal stability of the model increased instead of decreasing as that of tailless airplanes with swept-back wings usually does.

3. Power caused a slight reduction in the longitudinal stability measured at constant power. This reduction in stability, however, did not affect the longitudinal steadiness of the model in flight tests.

4. The model did not show the tendency to trim at very high angles of attack (above the stall) that has been a characteristic of some swept-back tailless airplanes.

5. The lateral flight characteristics of the model with both vertical tails installed were good. The directional stability of the model was satisfactory and was improved by the application of power. The effective dihedral was desirably small and was not appreciably affected by power.

6. The control surfaces of the model provided adequate longitudinal and lateral control.

Langley Memorial Aeronautical Laboratory
National Advisory Committee for Aeronautics
Langley Field, Va.

REFERENCES

1. Stability Research Division: An Interim Report on the Stability and Control of Tailless Airplanes. NACA ACR No. L4H19, 1944.

2. Jones, Robert T.: Notes on the Stability and Control of Tailless Airplanes. NACA TN No. 837, 1941.

3. Campbell, John P., and Seacord, Charles L., Jr.: Determination of the Stability and Control Characteristics of a Tailless All-Wing Airplane Model with Sweepback in the Langley Free-Flight Tunnel. NACA ACR No. L5A13, 1945.

4. Trouncer, J., and Wright, D. F.: Wind Tunnel Tests on the Effect of Variable Incidence Tips and Tip Slats on Tailless Gliders. TN No. Aero 1496, British R.A.E., Aug. 1944.

5. Shortal, Joseph A., and Osterhout, Clayton J.: Preliminary Stability and Control Tests in the NACA Free-Flight Wind Tunnel and Correlation with Full-Scale Flight Tests. NACA TN No. 810, 1941.

6. Shortal, Joseph A., and Draper, John W.: Free-Flight-Tunnel Investigation of the Effect of the Fuselage Length and the Aspect Ratio and Size of the Vertical Tail on Lateral Stability and Control. NACA ARR No. 3D17, 1943.

7. Zimmerman, C. H.: Preliminary Tests in the NACA Free-Spinning Wind Tunnel. NACA Rep. No. 557, 1936.

8. House, Rufus O., and Wallace, Arthur R.: Wind-Tunnel Investigation of Effect of Interference on Lateral-Stability Characteristics of Four NACA 23012 Wings, an Elliptical and a Circular Fuselage, and Vertical Fins. NACA Rep. No. 705, 1941.

9. Campbell, John P., and Paulson, John W.: The Effects of Static Margin and Rotational Damping in Pitch on the Longitudinal Stability Characteristics of an Airplane as Determined by Tests of a Model in the NACA Free-Flight Tunnel. NACA ARR No. L4F02, 1944.

10. White, Maurice D.: Effect of Power on the Stick-Fixed Neutral Points of Several Single-Engine Monoplanes as Determined in Flight. NACA CB No. L4H01, 1944.

CONFIDENTIAL

TABLE I

FORCE TESTS OF STRAIGHT-WING, TAILLESS MODEL IN THE LANGLEY FREE-FLIGHT TUNNEL

Type of data	Configuration	Power	α (deg)	ψ (deg)	δ_e (deg)	δ_{a_R} (deg)	Figure
C_L, C_D, C_m against α	W	Off	Range	0	0	0	9
Do	F	---do---	---do---	0	-------	-------	9
Do	WF	---do---	---do---	0	0	0	9
Do	$WFPV_1V_2$	$T_c = 0$	---do---	0	0	0	9
Do	$WFPV_1V_2$	$T_c = 0$	---do---	0	0, -15	0	10, 12
Do	$WFPV_1V_2$	1200 bhp	---do---	0	0, -15	0	10, 12
C_n, C_l, C_Y against ψ	F	Off	8	Range	0	0	13
Do	WF	---do---	5	---do---	0	0	13, 15
Do	WFP	Windmilling	5	---do---	0	0	13, 15
Do	$WFPV_1$	---do---	5	---do---	0	0	13, 15
Do	$WFPV_1V_2$	---do---	5	---do---	0	0	13, 15
Do	$WFPV_1V_2$	---do---	12	---do---	0	0	13
Do	WFP	---do---	5	---do---	0	0	14
Do	WFP	1200 bhp	5	---do---	0	0	14
Do	$WFPV_1V_2$	$T_c = 0$	5	---do---	0	0	14, 15
Do	$WFPV_1V_2$	1200 bhp	5	---do---	0	0	14, 15
Do	$WFPV_1V_2$	2000 bhp	5	---do---	0	0	14, 15
C_l, C_n against δ_{a_R}	$WFPV_1V_2$	Windmilling	4, 8, 12	0	0	Range	16

NATIONAL ADVISORY COMMITTEE FOR AERONAUTICS

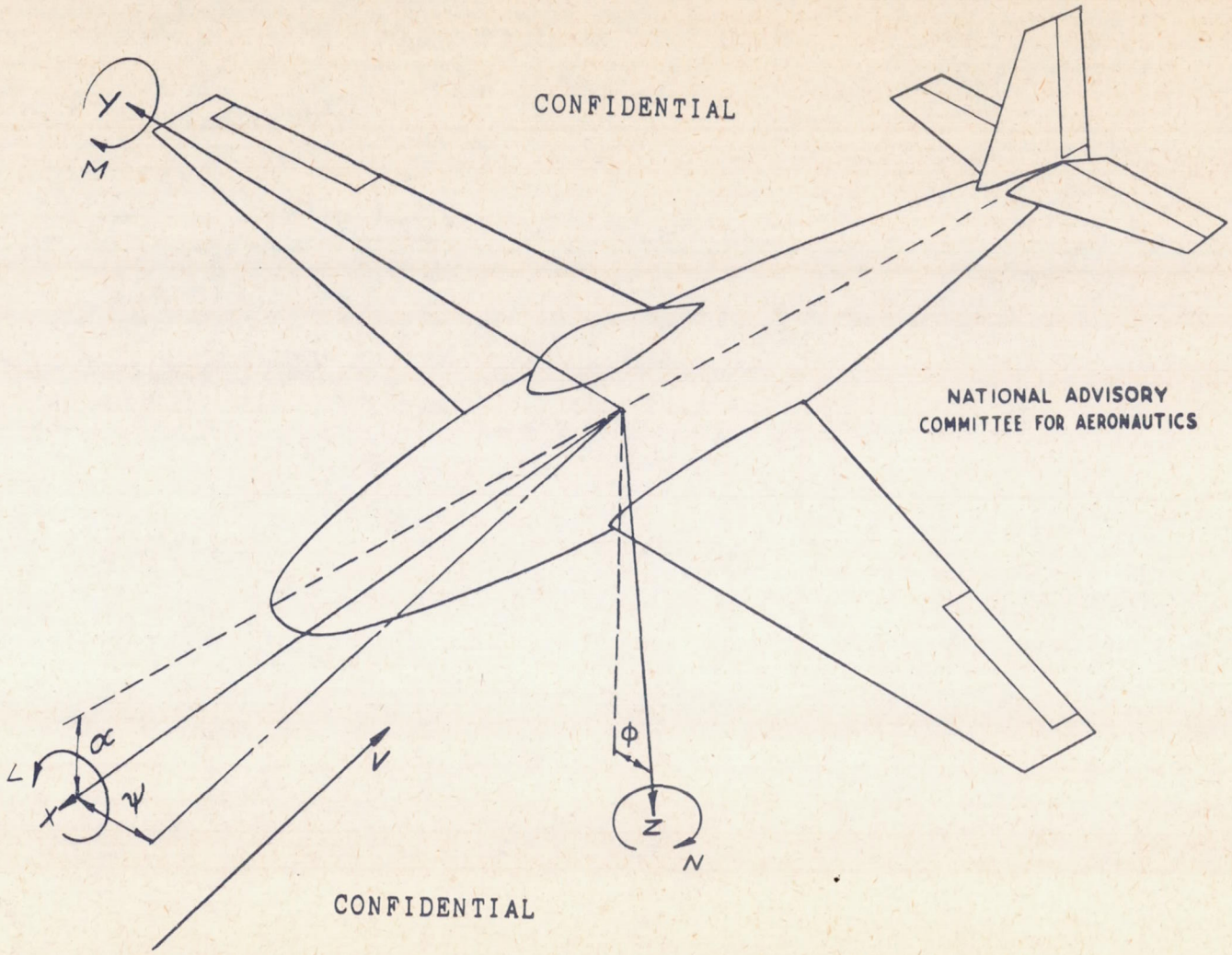

Figure 1.- System of stability axes. Arrows indicate positive direction of moments and forces.

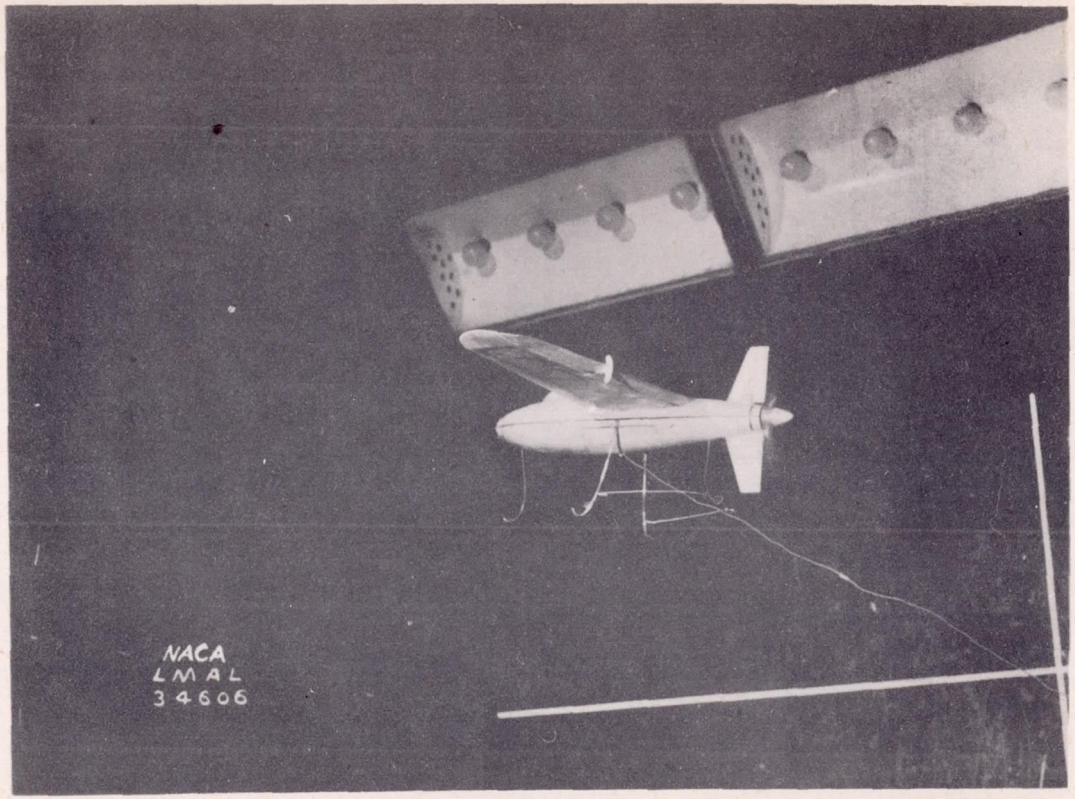

Figure 2.- Test section of Langley free-flight tunnel showing model in flight.

CONFIDENTIAL

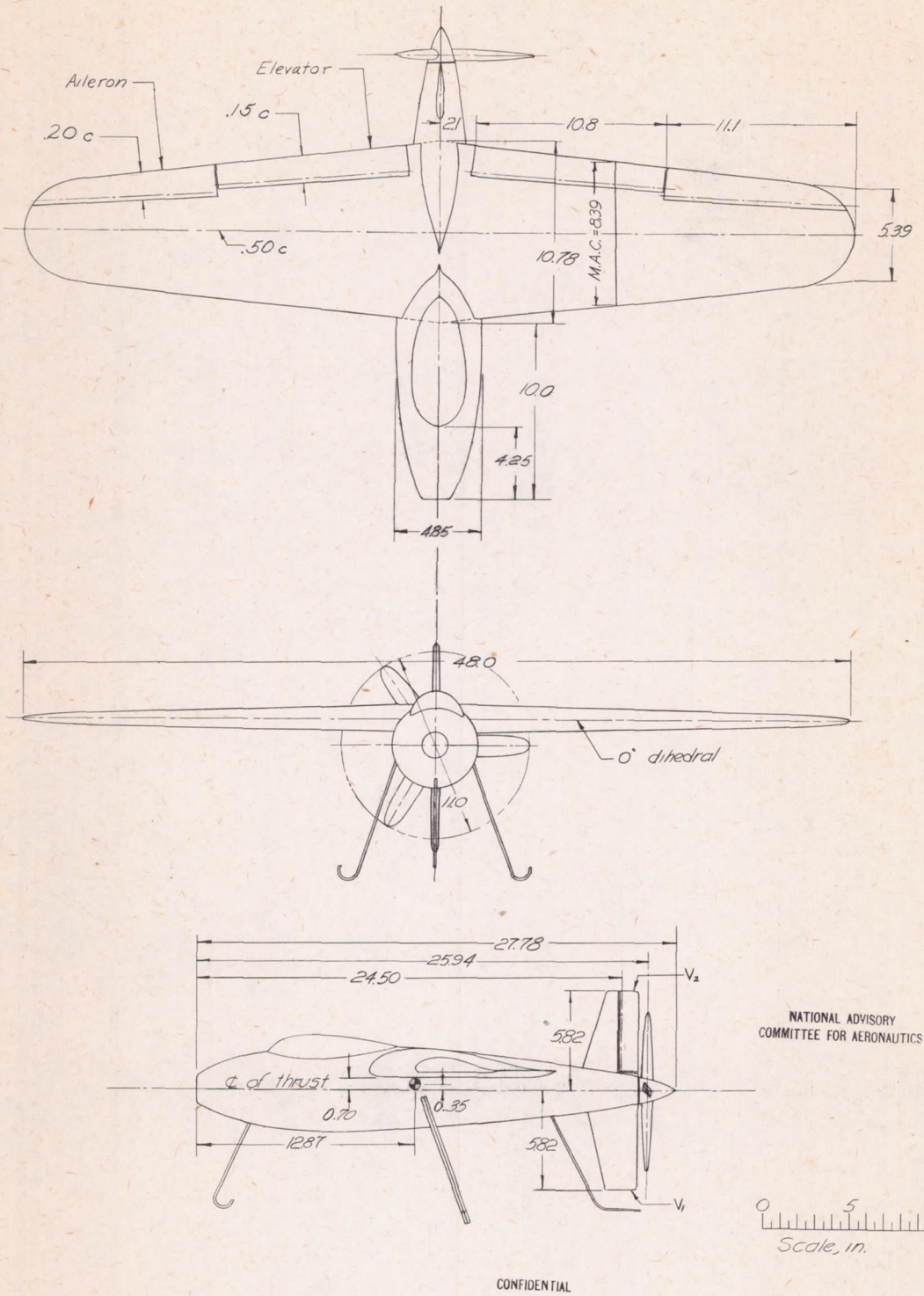

CONFIDENTIAL

Figure 3. — Drawing of $\frac{1}{10}$ scale straight-wing, tailless fighter model tested in the Langley free-flight tunnel.

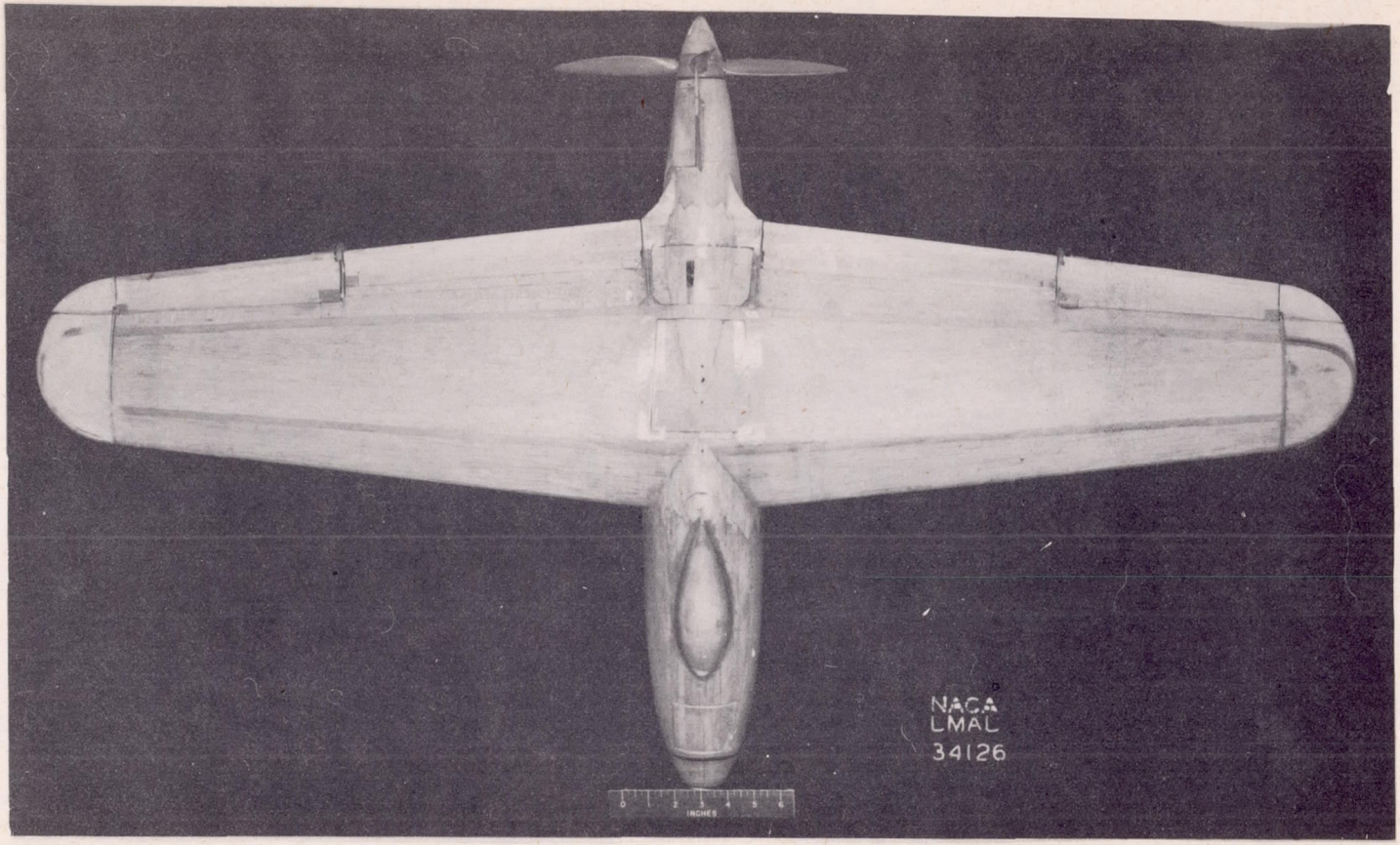

Figure 4.- Plan view of straight-wing, tailless fighter model tested in the Langley free-flight tunnel.

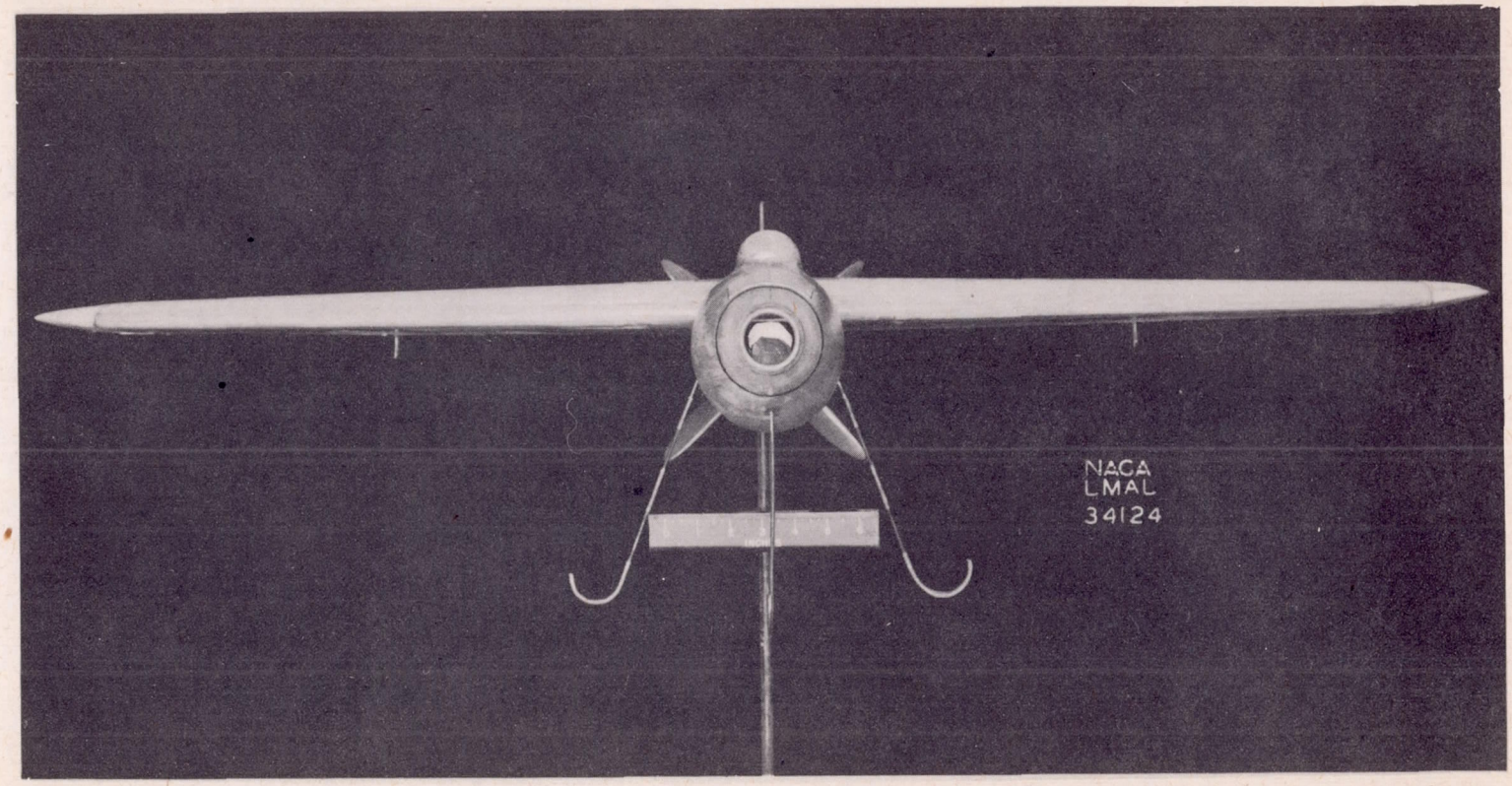

Figure 5.- Front view of straight-wing, tailless fighter model tested in the Langley free-flight tunnel.

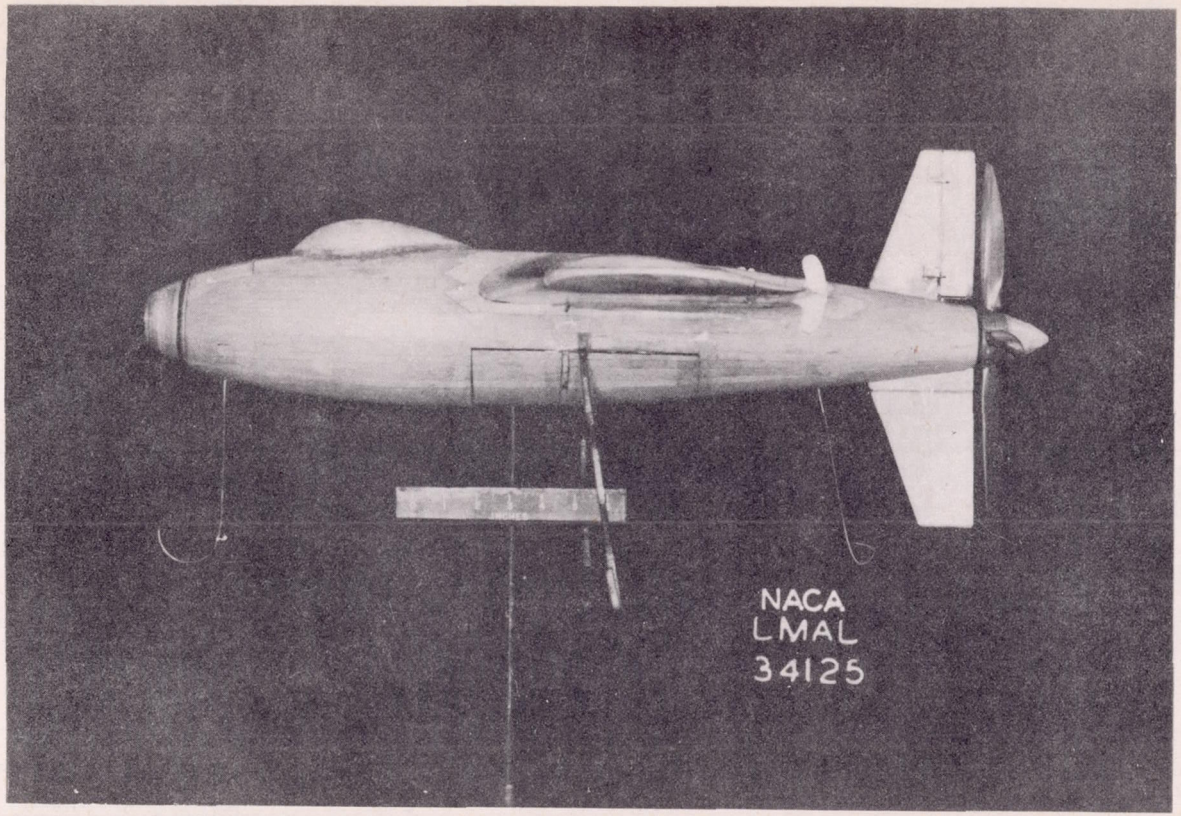

Figure 6.- Side view of straight-wing, tailless fighter model tested in the Langley free-flight tunnel.

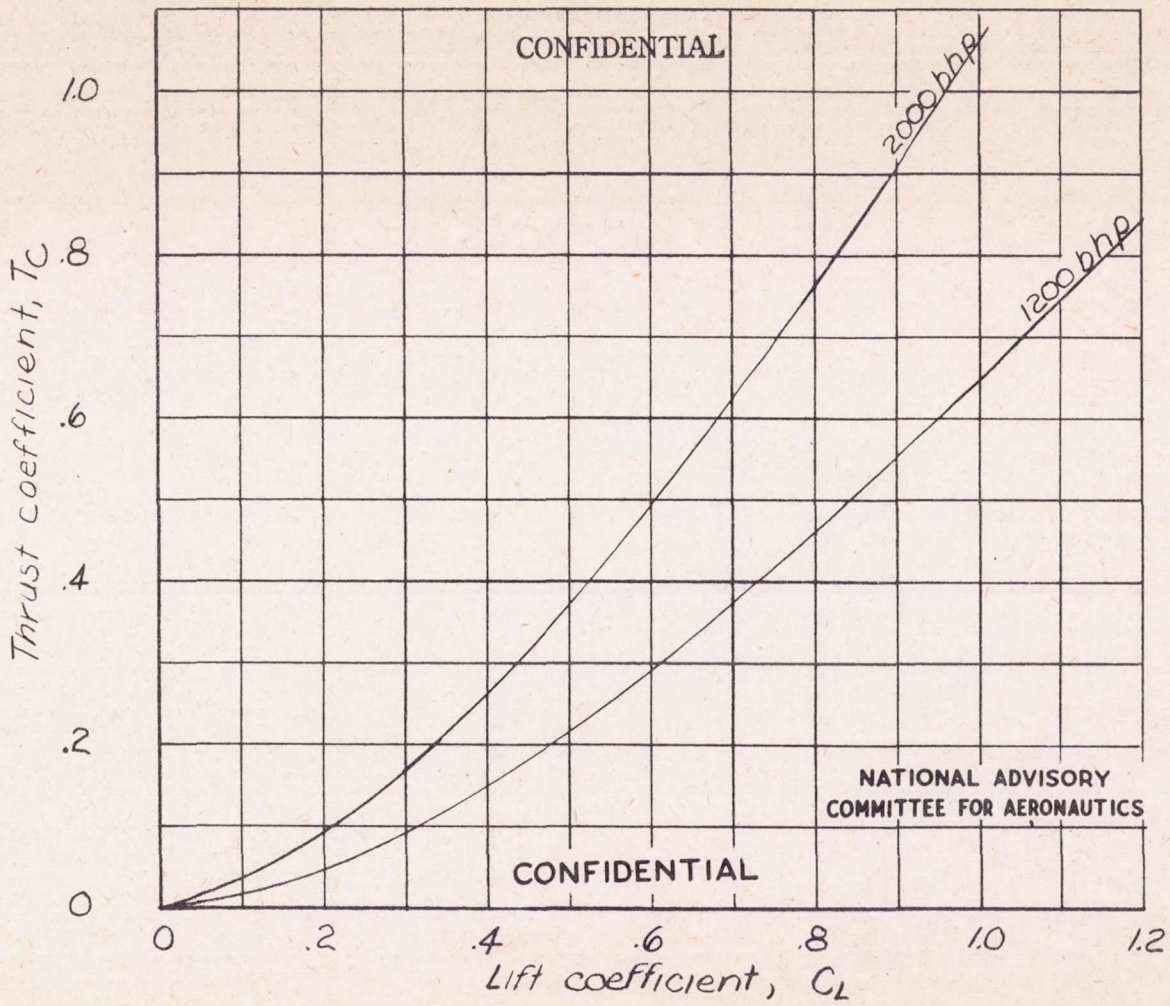

Figure 7.- Curves of thrust coefficient against lift coefficient for the straight-wing, tailless fighter model tested in the Langley free-flight tunnel.

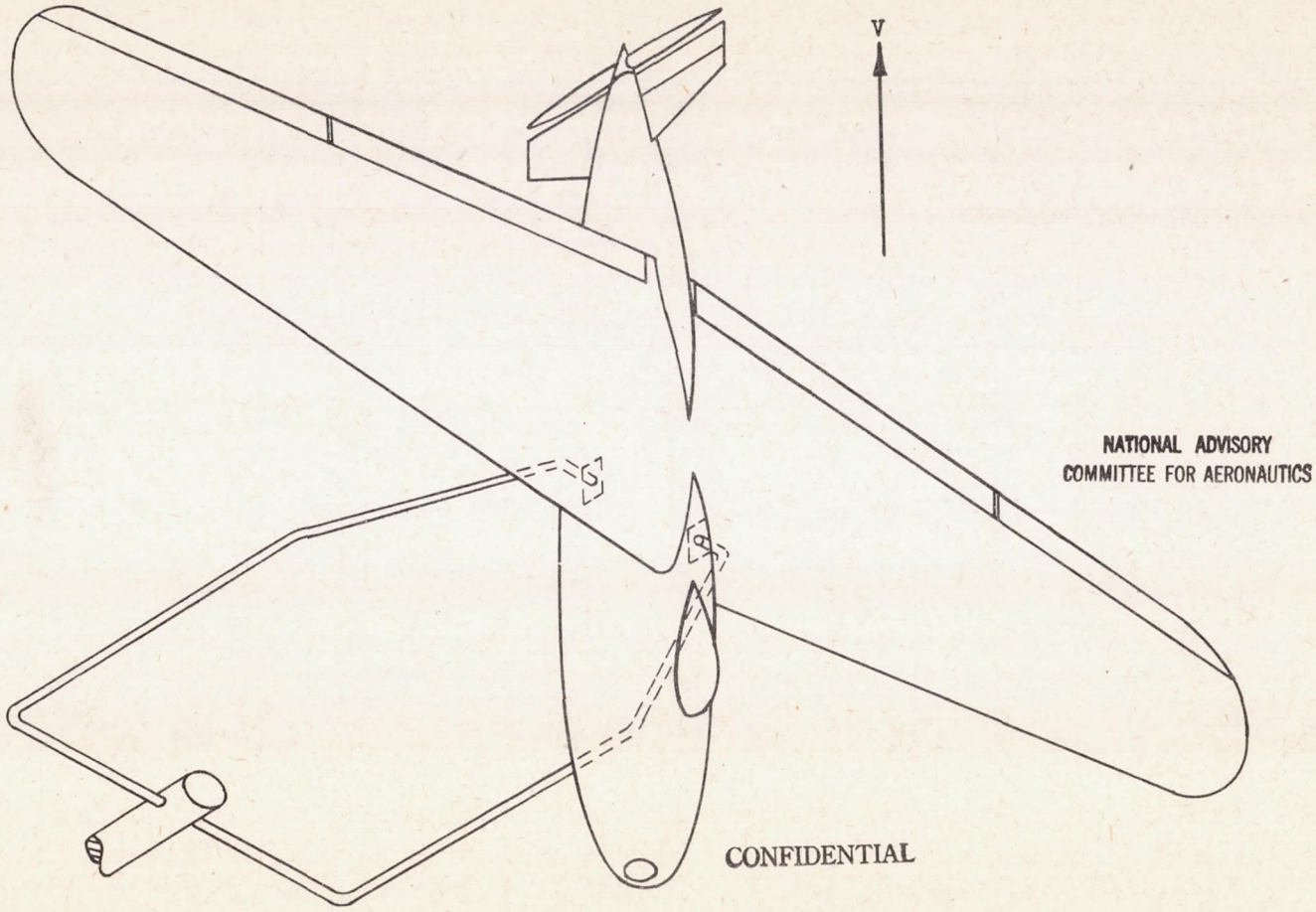

Figure 8.- Model mounted on free-to-trim stand in Langley 15-foot free-spinning tunnel. Model is free to pitch at center of gravity.

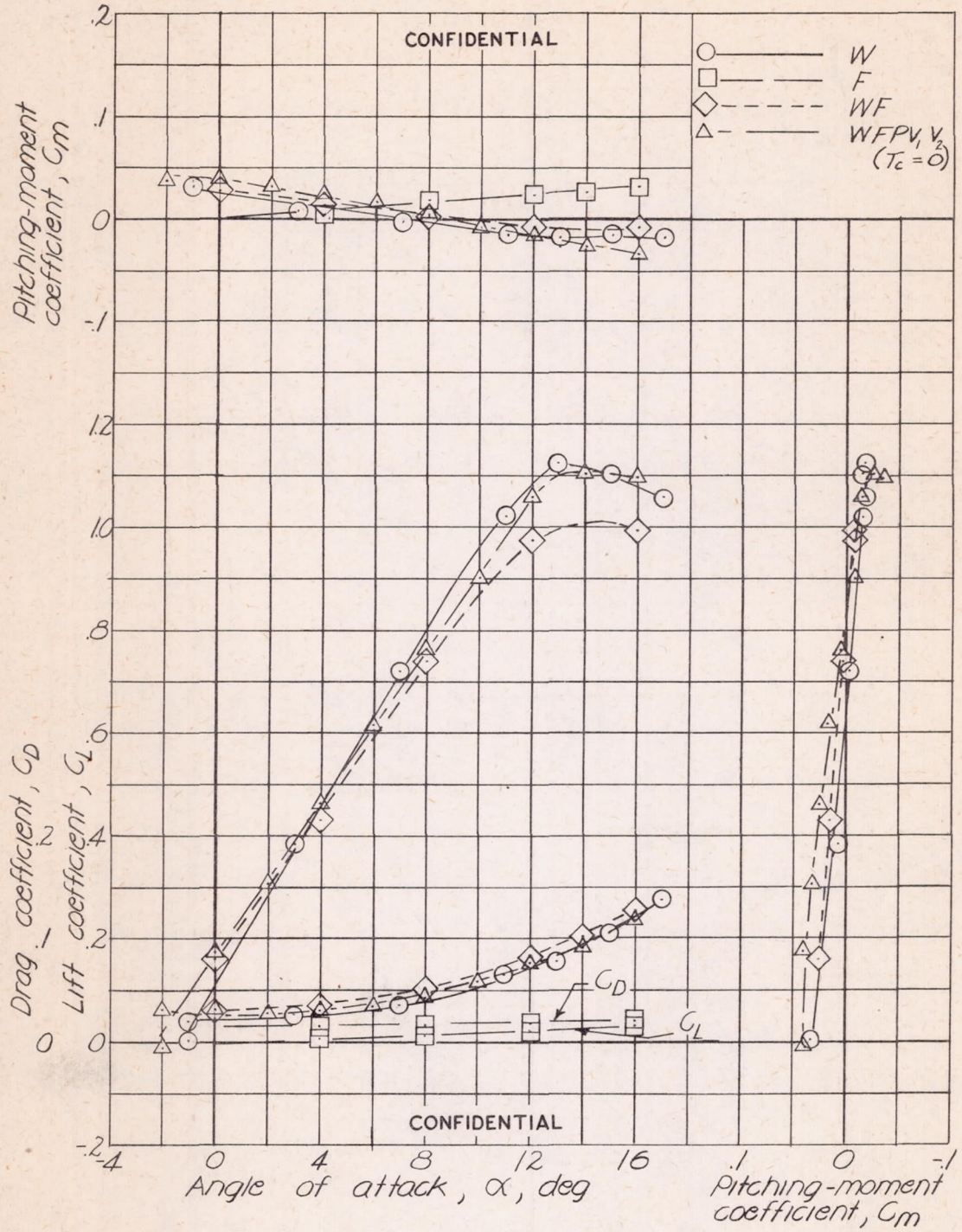

Figure 9.- Aerodynamic characteristics of straight-wing, tailless fighter model and its component parts tested in Langley free-flight tunnel. Center-of-gravity location, 0.20 M.A.C.; q, 4.09 pounds per square foot.

NATIONAL ADVISORY COMMITTEE FOR AERONAUTICS

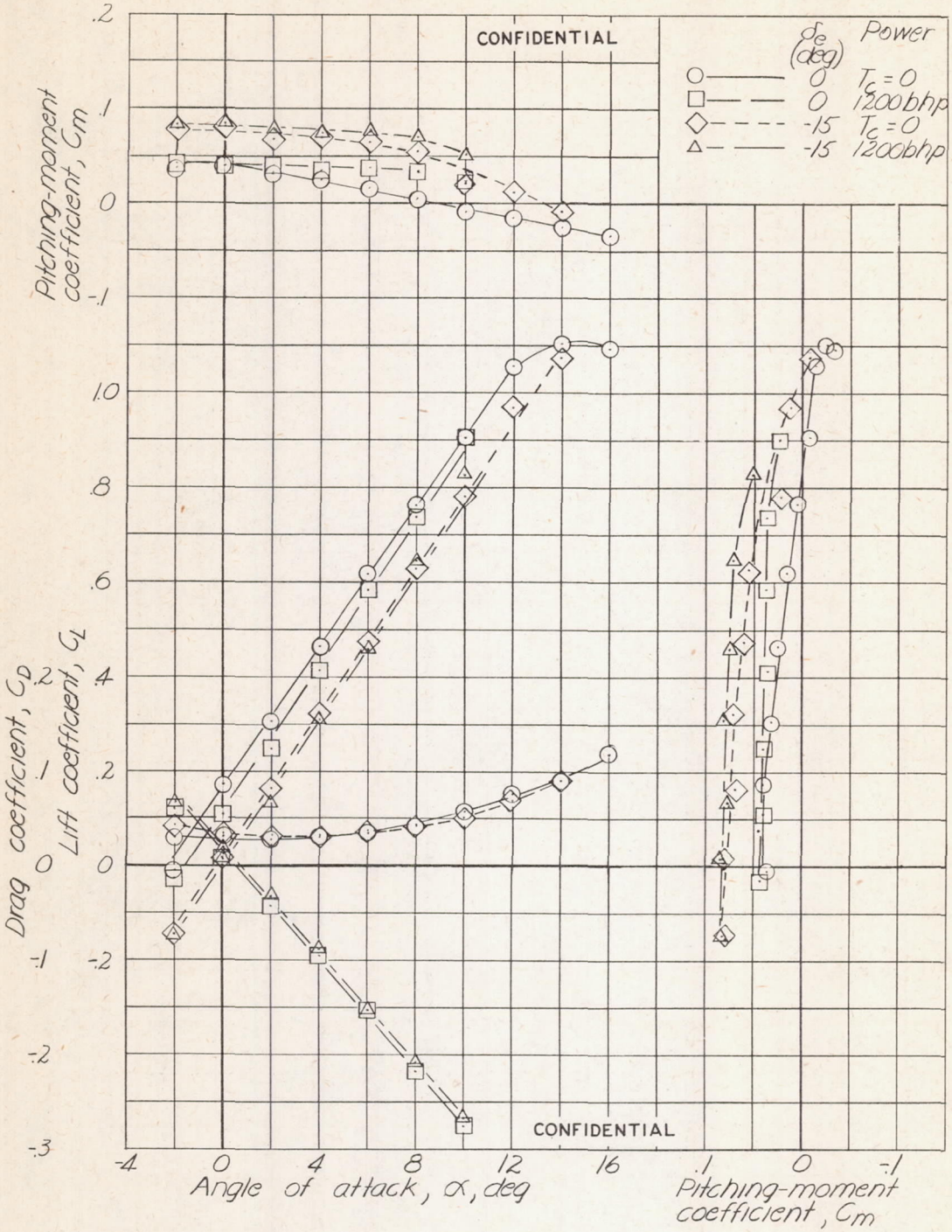

Figure 10.- Effect of power on longitudinal characteristics of straight-wing, tailless fighter model tested in Langley free-flight tunnel. Center-of-gravity location, 0.048 $\bar{c}$ above thrust line and at 0.20 M.A.C.; q, 4.09 pounds per square foot.

NATIONAL ADVISORY COMMITTEE FOR AERONAUTICS

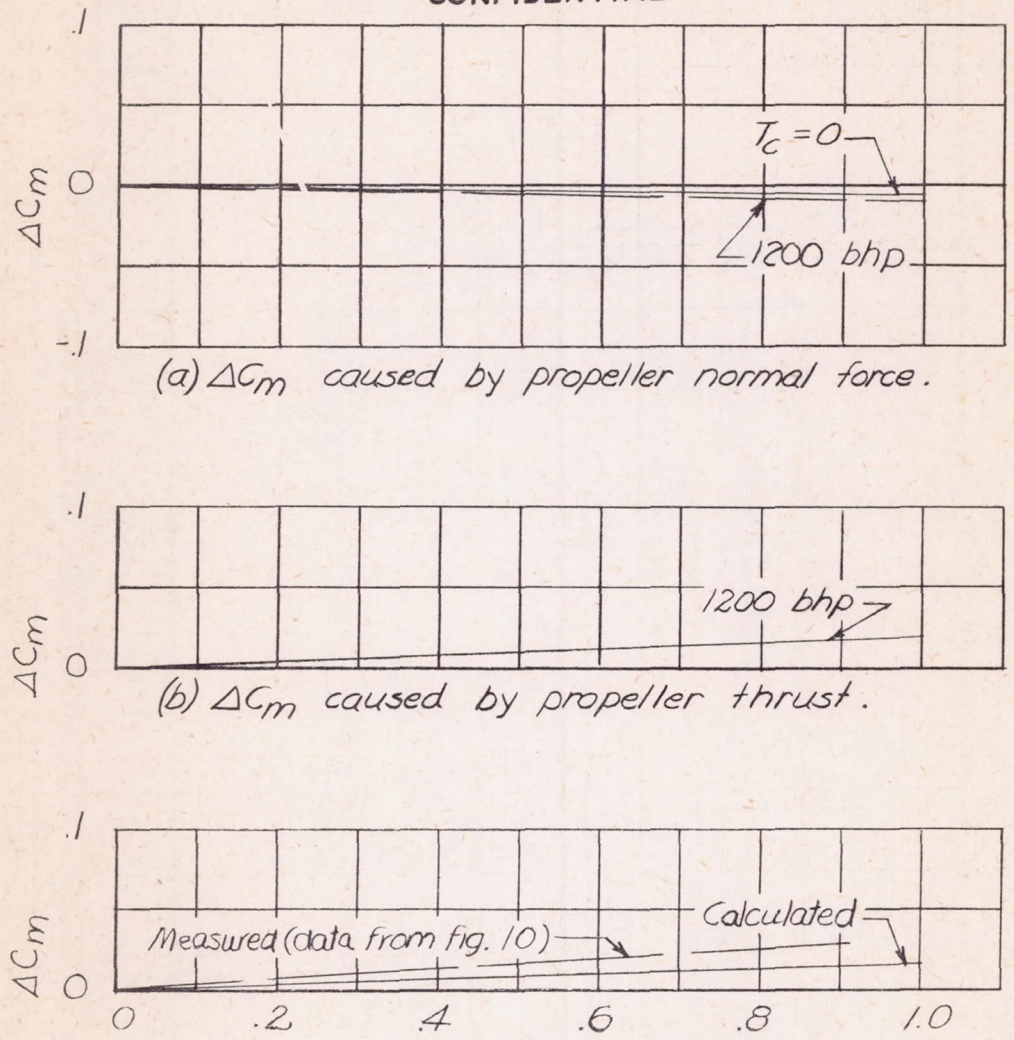

NATIONAL ADVISORY COMMITTEE FOR AERONAUTICS

Figure 11.- Effect of propeller forces on the longitudinal stability of the straight-wing, tailless fighter model tested in the Langley free-flight tunnel. Center-of-gravity location, 0.20 M.A.C. and 0.048 $\bar{c}$ above thrust line.

CONFIDENTIAL

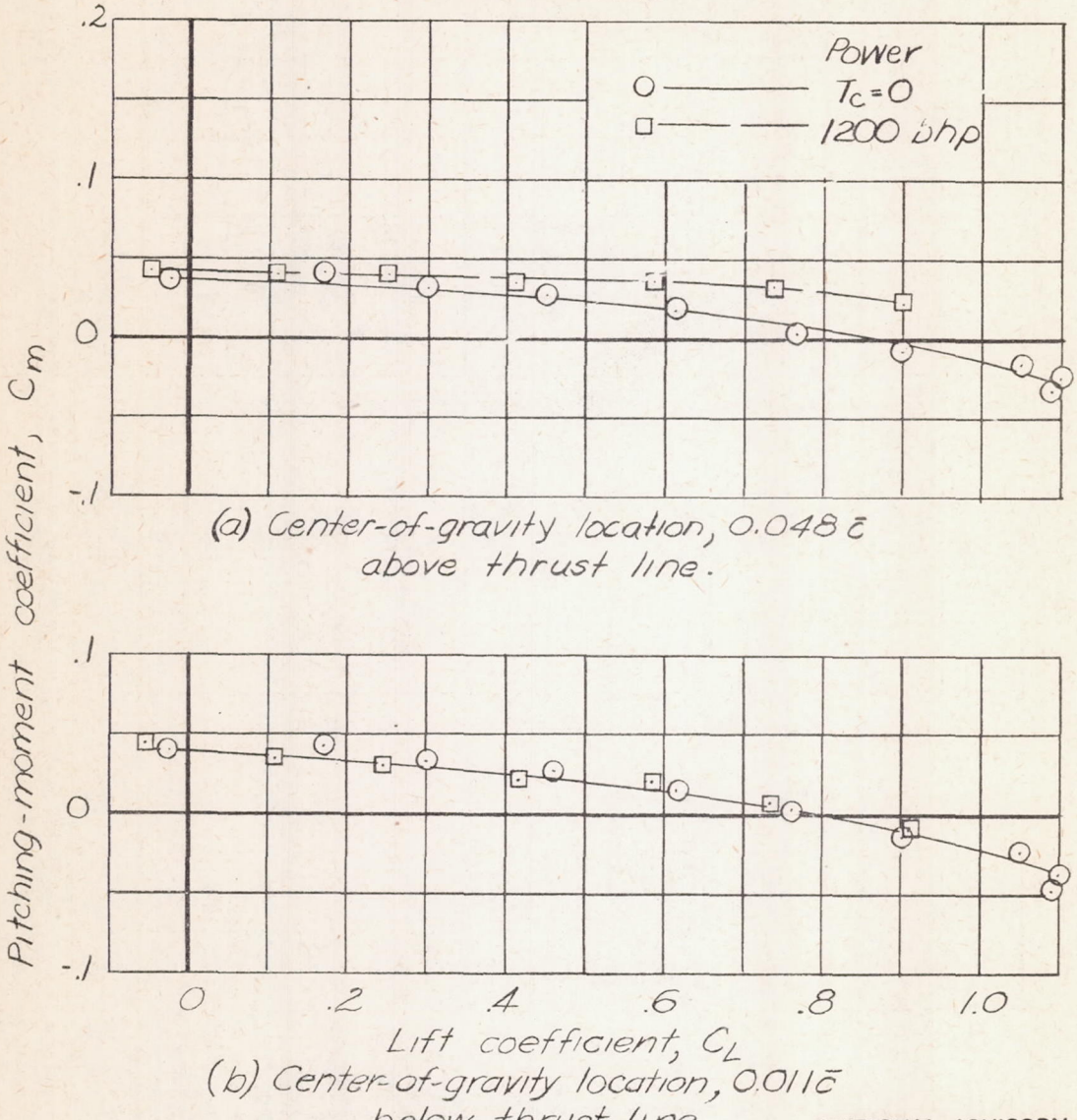

(a) Center-of-gravity location, 0.048 $\bar{c}$ above thrust line.

(b) Center-of-gravity location, 0.011 $\bar{c}$ below thrust line.

NATIONAL ADVISORY COMMITTEE FOR AERONAUTICS

Figure 12.- Comparison of the effects of power for two center-of-gravity locations. Data from tests of straight-wing, tailless fighter model in the Langley free-flight tunnel. Center-of-gravity location, 0.20 M.A.C.

CONFIDENTIAL

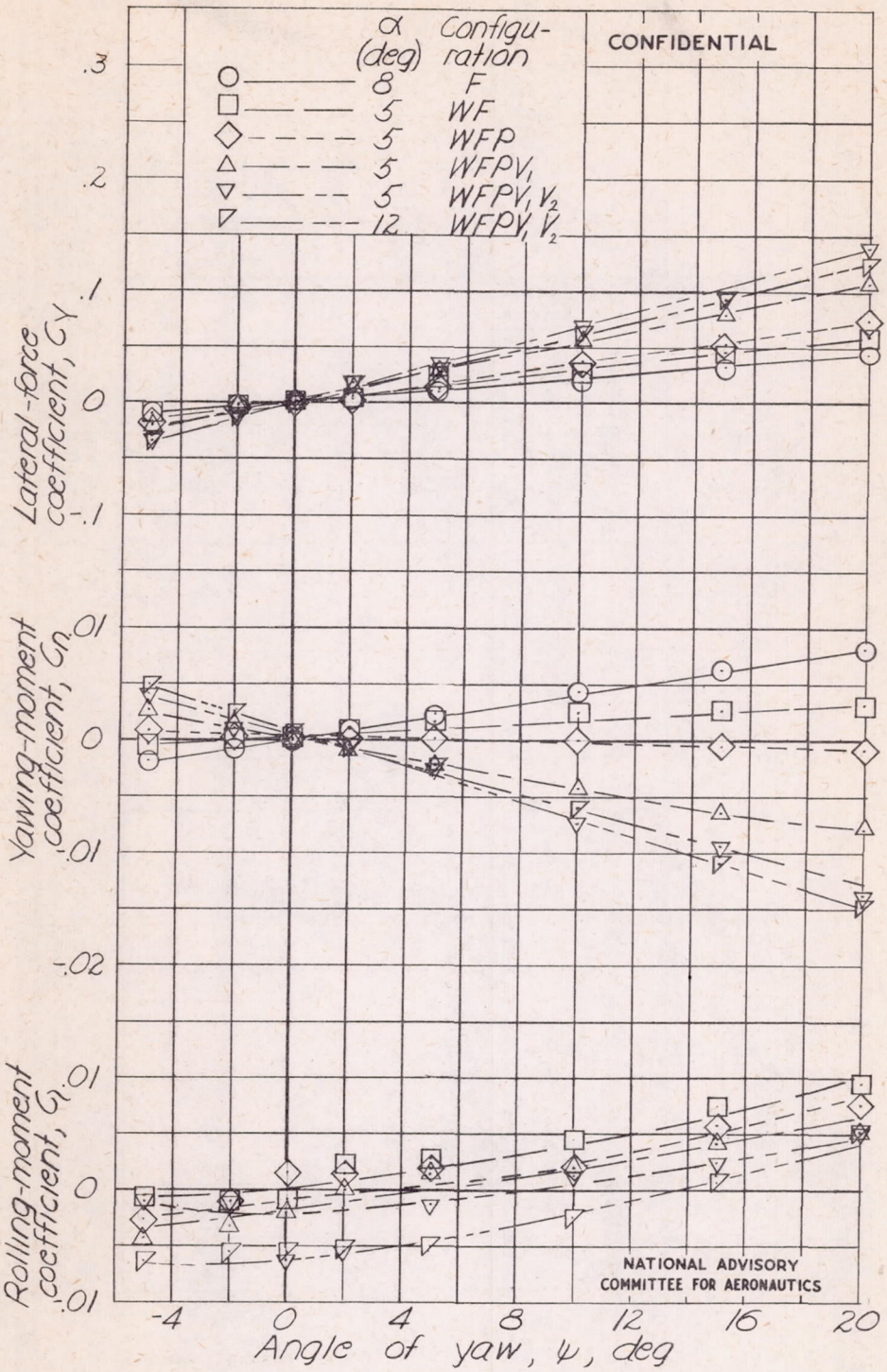

Figure 13.- Lateral stability characteristics of straight-wing, tailless fighter model tested in Langley free-flight tunnel. q, 4.09 pounds per square foot; four-blade propeller.

CONFIDENTIAL

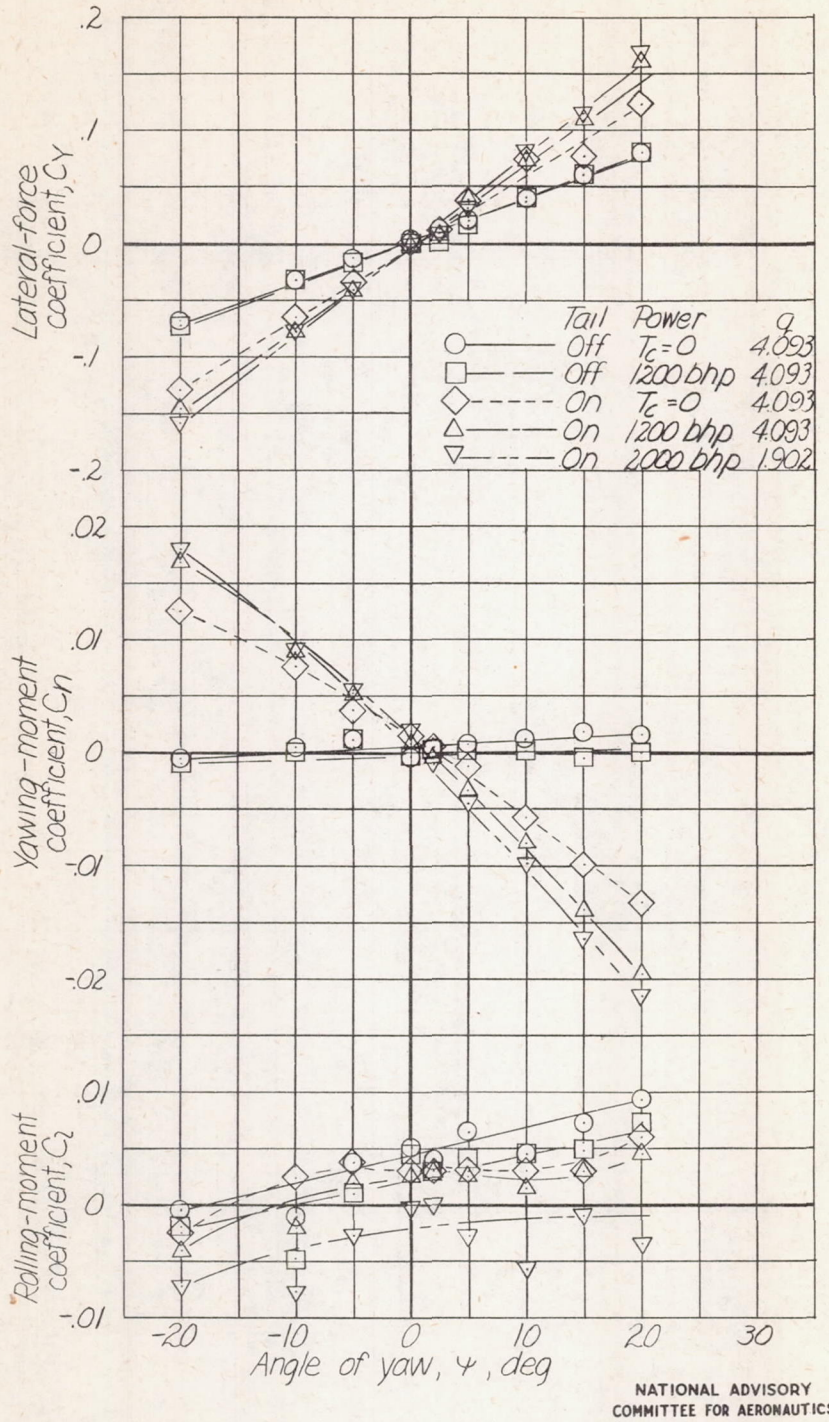

Figure 14.- Effect of power on lateral stability characteristics of straight-wing, tailless fighter model tested in the Langley free-flight tunnel. $\alpha = 5°$; $C_L = 0.5$.

CONFIDENTIAL

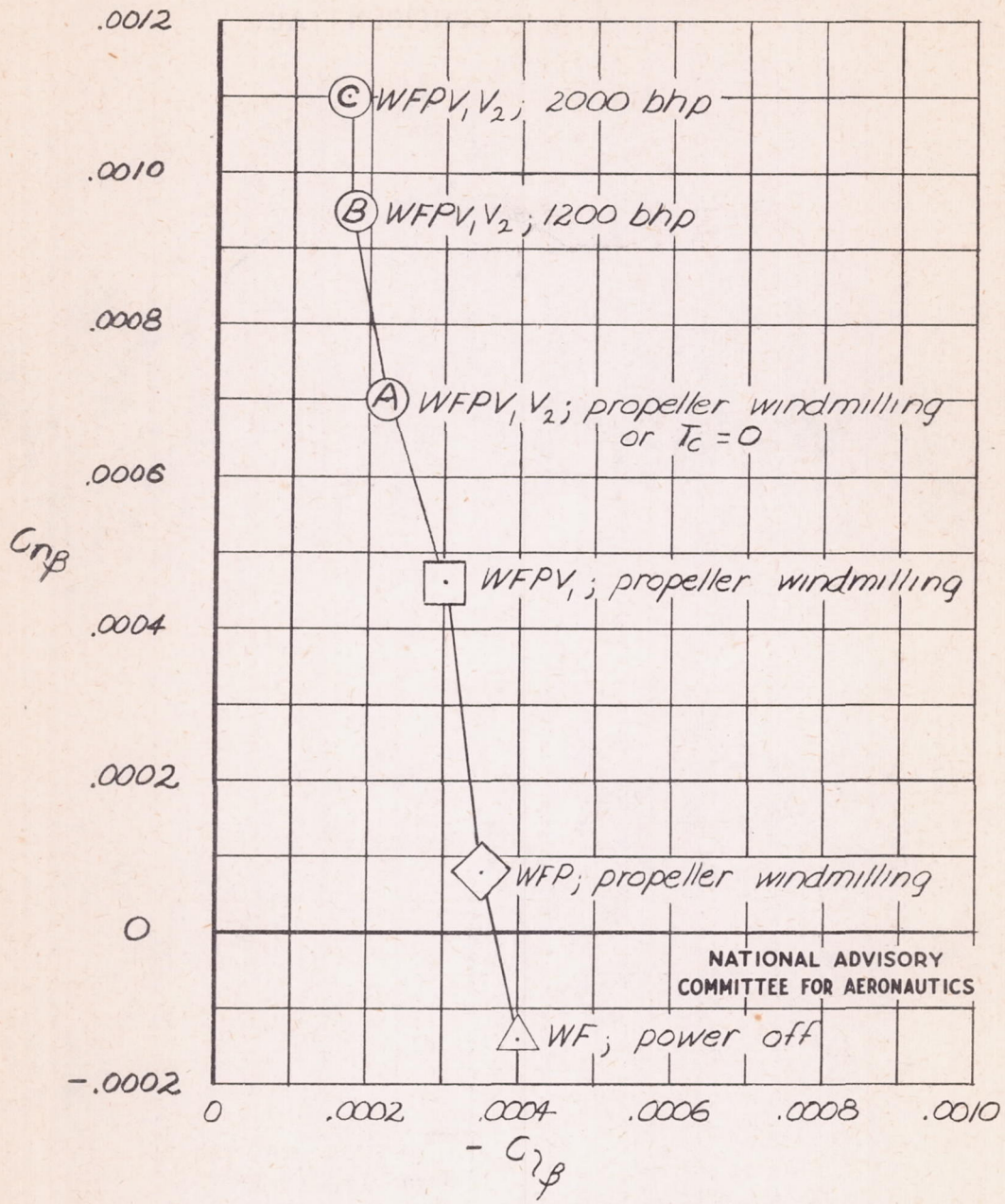

Figure 15.- Values of lateral-stability parameters C_{n_β} and C_{l_β} for various configurations of the straight-wing, tailless fighter model tested in the Langley free-flight tunnel.

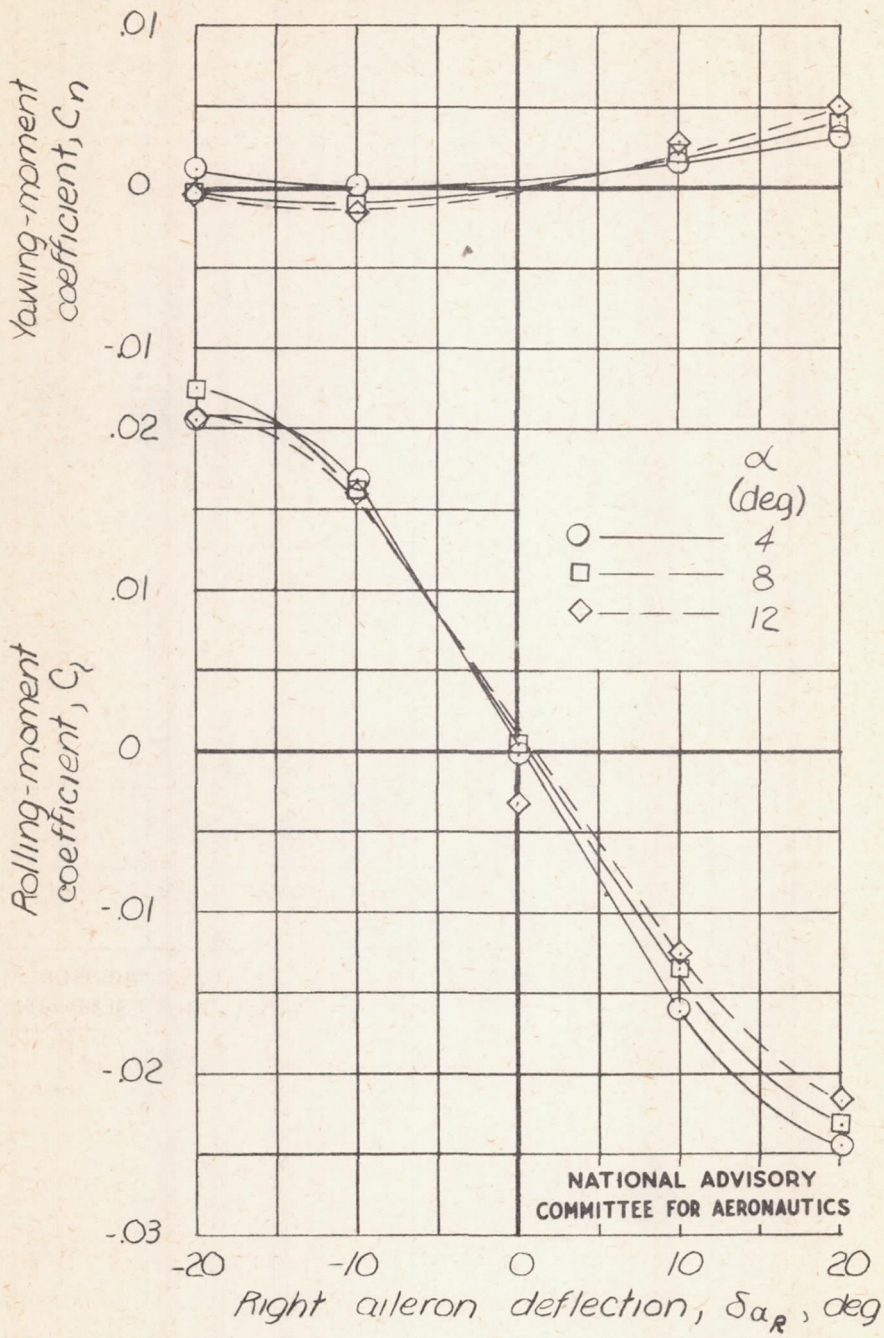

Figure 16.- Aileron effectiveness of straight-wing, tailless fighter model tested in Langley free-flight tunnel.